Self-Powered and Light-Adaptable Stretchable Electrochromic Display

Wenting Wu, Wei Church Poh, Jian Lv, Shaohua Chen, Dace Gao, Fei Yu, Hui Wang, Huajing Fang, Hong Wang,* and Pooi See Lee**

A stretchable electrochromic display with a self-powered feature is an attractive concept in addressing the demands of information visualization and interaction without an external power supply for next-generation wearable and portable electronics. Herein, a self-powered stretchable electrochromic display is proposed for the first time, with WO_3 on the stretchable conductor as the electrochromic electrode integrated in parallel with the Zn/carbon electrodes and topped with a $ZnCl_2$-based organohydrogel. This geometrically designed electrochromic device can be self-colored by the chemical potential gap between WO_3/Zn electrodes. The self-bleaching process caused by the oxidation of the reduced WO_3 electrode is facilitated by the leakage current between the WO_3/carbon electrodes. In this constructed self-powered system, the electrochromic electrode shows reversible coloring/bleaching performance up to 50% strain and maintains favorable stability with power-free reversible electrochemical switching for 400 cycles. Optical contrast retention at 81% is maintained for 200 stretching/recovery cycles. The prepared device combined with a phosphorescent substrate is demonstrated as a light-adaptable stretchable display, where the "on/off" states of the display are shown in both bright and dark conditions without power consumption. This work provides broad application prospects for futuristic multifunctional stretchable and portable display electronics.

1. Introduction

Stretchable electrochromic displays, as emerging soft electronics, enabling information visualization and interaction such as smart wearables and electronic skins, have huge potential for applications in next-generation electronics.[1,2] Endowing the typical electrochromic electrodes with stretchability is technically more challenging than that with flexibility. This is because stretchable electrochromic electrodes not only need to endure tensile or shear deformation of the electrode but also require stable electrochemical reactions upon stretching for satisfactory electrochromic performances.[3] Among these reported high-performance stretchable electrochromic electrodes,[1,4–8] the key strategies for fabricating these electrodes are to design microstructures capable of stretching and to ensure high mechanical and chemical compatibility between the conductor and electrochromic layer. For instance,[4] the construction of Au/Ag core-shell nanowires embedded in polydimethylsiloxane (PDMS) conductor provides high oxidation and deformation resistance, capable of showing a good electrochromic performance by coating bistacked WO_3 nanotube/ poly(3,4-ethylenedioxythiophene)-poly(styrene sulfonate) (PEDOT:PSS) layer under the strain of 0–20%. And the electrochromic electrodes with simplified interface constructed by PEDOT/polyurethane (PU)[7] and PEDOT:PSS/thermoplastic PU (TPU)[1] exhibit stable electrochromic performance upon stretching. Moreover, by assembling anti-cylindrical photonic crystals with shape memory alloy composites, the obtained electrochromic electrode with high integration can dynamically change colors upon stretching.[8] In most cases, silver nanowires (AgNWs) and PDMS are used as conductive materials and elastic substrates for stretchable conductors.[9–11] For instance, a wrinkled AgNWs network in the PDMS substrate was demonstrated to improve the tensile properties of the conductor.[10] The embedment of AgNWs in PDMS has also been obtained, achieving conductors with high tolerance to tensile deformation.[11] To integrate the conductor well with the electrochromic layer, a wrapping structure/protection layer can be designed inside the electrochromic electrode. For example, the WO_3@AgNWs core-shell structure

---

W. Wu, W. C. Poh, J. Lv, S. Chen, D. Gao, F. Yu, H. Wang, P. S. Lee
School of Materials Science and Engineering
Nanyang Technological University
Singapore 639798, Singapore
E-mail: pslee@ntu.edu.sg

W. Wu, H. Fang
State Key Laboratory for Mechanical Behavior of Materials
School of Material Science and Engineering
Xi'an Jiaotong University
Xi'an 710049, China
E-mail: fanghj@xjtu.edu.cn

H. Wang
Department of Materials Science and Engineering
Southern University of Science and Technology
Shenzhen 518055, China
E-mail: wangh6@sustech.edu.cn

The ORCID identification number(s) for the author(s) of this article can be found under https://doi.org/10.1002/aenm.202204103.

DOI: 10.1002/aenm.202204103

prevents the delamination and oxidation of the electrode,[5] and the PEDOT:PSS protection layer improves the conductivity and adhesion between layers and antioxidation of the electrode.[4,6,12] The above strategies suggest that the AgNWs/PDMS-based conductor with an electrochromic layer is an attractive candidate for stretchable electrochromic devices. Typically, stretchable electrochromic devices require the input of an external power supply, restricting the development of devices' portability and autonomous deployment.[13] In this regard, imparting the stretchable electrochromic device with self-powered ability is urgently needed.

To date, several pioneering works have successfully developed self-powered electrochromic devices by utilizing the internal chemical potential to drive electrochromic behaviors.[14–16] The underlying reason for the self-powered ability of electrochromic devices attributes to the low potential and low energy consumption attributes, which fit well with the chemical potential supplying traits. Conventionally, the internal chemical potential is built by the work function difference between the electrochromic electrode and an active metal electrode (such as Al,[17] Zn,[18] Fe,[19] and Mg[20]). For example, Wang et al. reported a self-powered Prussian blue (PB)/Al electrochromic device. The chemical potential difference between PB/Al electrodes drives the self-bleaching behavior simply by connecting the two electrodes. During disconnection of the PB/Al electrodes, the O_2 involves in the chemical oxidation reaction of Prussian white (PW) to PB, leading to self-coloration.[14] A similar self-powered electrochromic system was also constructed in the high-capacity $WO_{2.72}$/Al electrochromic battery.[16] It is also shown that by adding a trace amount of H_2O_2 into the system, the self-bleaching/charging process is accelerated due to the enhanced chemical potential difference between reduced tungsten oxide/H_2O_2. However, this strategy of adding oxidants is not suitable for sealed/portable devices due to safety concerns. To resolve this problem, additional counter electrodes (Pt/carbon cloth/etched carbon paper) can be introduced to facilitate faster oxidation processes in self-powered electrochromic systems.[19,21,22] In these multielectrode systems, the chemical potential difference between the complementary electrode and the reduced electrochromic electrode promotes the oxidation process. Therefore, the rational design of device configuration for the self-powered electrochromic system is expected to show favorable and stable electrochromic performances.

In this work, we demonstrate a self-powered stretchable electrochromic display by integrating the Zn/carbon electrodes with the WO_3 electrochromic electrode on the highly conductive and stable PEDOT:PSS/AgNWs/PDMS stretchable conductor. Assembled with an organohydrogel, the WO_3-based stretchable electrochromic electrode can be self-colored when connecting with the Zn electrode driven by the internal chemical potential. When disconnecting the WO_3/Zn electrodes, the self-bleached state is achieved within 60 s owing to the oxidation of the reduced WO_3 electrode by O_2 and facilitated by the leakage current inside the WO_3/ carbon cloth electrodes. Reversible and stable electrochromic performances are obtained upon stretching (0–50% strain) and 200 stretching/recovery cycles; the electrochemical stability is also proved in 400 coloring/bleaching cycles without any electrical input, signifying zero energy consumption. In particular, a light-adaptable and self-powered stretchable electrochromic display is fabricated by combining the device with a phosphorescent substrate. "On/off" states of the display are exhibited without an external power source in both bright and dark conditions, indicating promising applications in multifunctional portable and stretchable electronics.

2. Results and Discussion

2.1. Concept and Design of the Self-Powered Stretchable Electrochromic Display

The schematic illustration of the stretchable electrochromic display is shown in **Figure 1**. The stretchable electrochromic electrode consists of multilayers: the conductive AgNWs are embedded into the elastomeric PDMS substrate as the current collector; then a conductive polymer PEDOT:PSS layer is coated on it to form the stretchable conductor, aiming to improve the conductivity while protecting the AgNWs during mechanical stretching. WO_3 is used as the cathodic electrochromic material, which has been well-studied for its electrochromic performances upon ions/electrons insertion/extraction.[23] The patterned WO_3 is spray-coated on top of the PEDOT:PSS/AgNWs/PDMS conductor as the electrochromic electrode.

To fabricate the electrochromic display, the WO_3-based stretchable electrochromic electrode is assembled in parallel configuration with the carbon cloth and zinc electrode. A stretchable $ZnCl_2$-Ethylene glycol (EG)/H_2O-Polyvinyl alcohol (PVA) organohydrogel electrolyte is integrated with these electrodes, forming the top layer of the device. The Zn electrode is chosen as the counter electrode to connect with the electrochromic electrode for self-coloring, and the carbon cloth is used to induce the self-bleaching process. Specific mechanisms will be elucidated in the following discussion. The "on/off" (self-colored/bleached) states of the electrochromic display are expected to be realized when the WO_3 electrode is connected/disconnected with the Zn electrode.

2.2. Microstructure and Electrical Properties of the Stretchable Electrode

The as-prepared PEDOT:PSS layer coated on the AgNWs-embedded PDMS is serving as the stretchable conductor and is further investigated as shown in **Figure 2**a,b. The AgNWs are released from the glass substrate to the PDMS substrate by our previously reported method.[12] This method provides strong interactions between AgNWs and PDMS substrate resulting in the high transfer efficiency of AgNWs and satisfactory conductivity of the AgNWs/PDMS conductor. The surface morphology from scanning electron microscope (SEM) analysis (Figure 2a) of the conductor indicates that AgNWs are partially protruding over the PDMS base for electrical conduction, which is the key component for the conductivity of the electrode. The sulfur element mapping (Figure 2b) confirms a homogenous distribution of the spray-coated PEDOT:PSS layer. The sheet resistance of the stretchable conductor without PEDOT:PSS is 14 Ω sq^{-1}, and the reduced sheet resistance of 12.3 Ω sq^{-1} is obtained

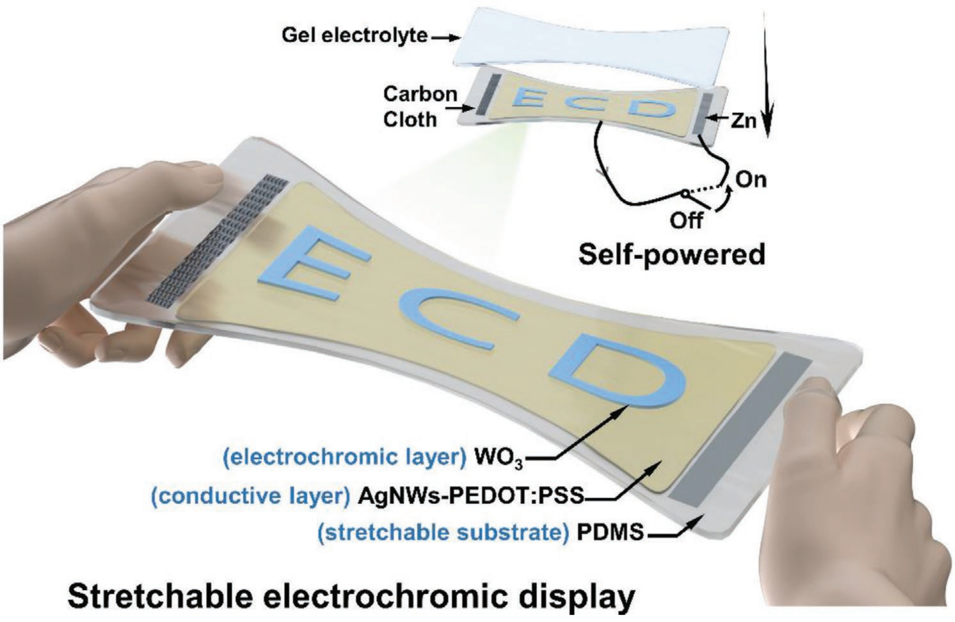

Figure 1. Schematic illustration of the self-powered stretchable electrochromic display.

after coating the thin conductive PEDOT:PSS layer. This value of resistance is comparable with commercial ITO glass or ITO/PET substrates.[24] The transmittance of the corresponding electrodes is slightly altered after coating the PEDOT:PSS layer, ranging from 70.9% to 70.5% @633 nm (Figure S1, Supporting Information). Besides, compared with the stretchable conductor without PEDOT:PSS, the relative resistance variation (R/R_0) of the stretchable conductor with PEDOT:PSS is smaller at various stretching strains (Figure 2c). In specific, the R/R_0 of the conductor with PEDOT:PSS increases to 15.8 at 70% strain, whereas that of the conductor without PEDOT:PSS reaches 128.9 at 70% strain. The PEDOT:PSS layer improves the electrical properties of the stretchable conductor because the additional PEDOT:PSS polymer can provide stable and effective conductive pathways between silver nanowires in the localized nanoscale domains during stretching.[25] During repeated peeling tests (Figure 2d), lower changes in resistivity can be observed with the PEDOT:PSS-coated stretchable conductor compared to its counterpart without PEDOT:PSS coating, indicative of a stronger adhesion between the AgNWs and PDMS substrate protected by the PEDOT:PSS layer. The combination of PEDOT:PSS/AgNWs/PDMS as a stretchable conductor, thereby, shows improved durability against mechanical stretching and peeling.

Subsequently, a layer of WO_3 is spray-coated onto the PEDOT:PSS/AgNWs/PDMS stretchable conductor to form the stretchable electrochromic electrode. SEM images in Figure 2e show that the WO_3 nanoparticles with a film thickness of

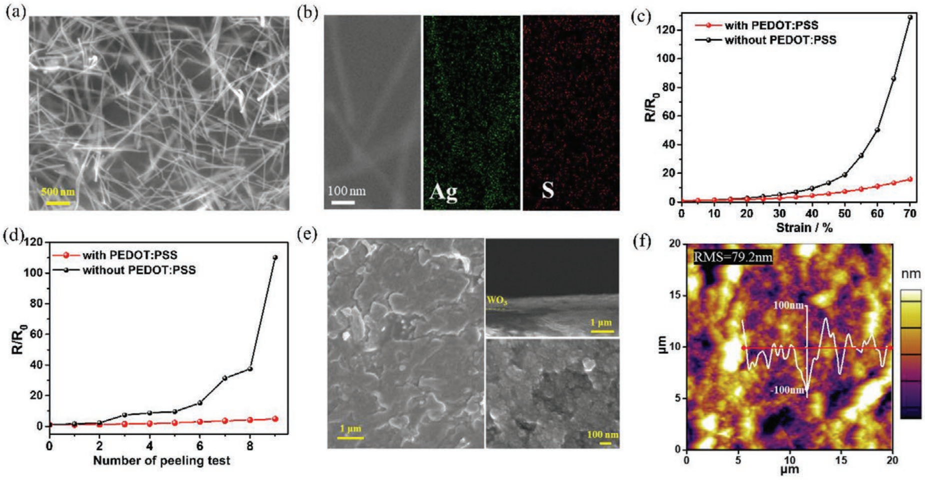

Figure 2. a) The surface morphology and b) element mapping of the PEDOT:PSS/AgNWs/PDMS stretchable conductors, the relative resistance variation of the stretchable conductors(with/without PEDOT:PSS) upon c) stretching test, and d) peeling test by scotch tape, e) the surface and cross-sectional morphologies of the WO_3 electrode, f) the AFM image of the WO_3 layer.

around 550 nm provide dense coverage on the conductor. From the Atomic Force Microscope (AFM) image in Figure 2f, the roughness of the WO_3 electrode is derived to be about 79.2 nm. This value is relatively large compared with other reported WO_3-based electrochromic films,[26] which could provide a larger surface area for the electrochemical reaction and ions intercalation.[27] And the thickness difference of the electrode is randomly distributed in the microscale regions, so it will not affect the uniformity of the colored state of the WO_3 electrode at a macroscopic visual perception. The chemical composition and phase structure of the WO_3 electrode are confirmed by the X-ray diffraction (XRD) measurement, as shown in Figure S2, Supporting Information. The additional hump around 25° indicates the existence of the amorphous phase of the WO_3 when compared with the bare conductive substrate.[28]

2.3. Moisture Retention Ability and Optical Properties of the Stretchable Gel Electrolyte

There is a growing interest in the use of hydrogel electrolytes in the electrochromic field due to their semi-solid properties and high conductivity.[29] Especially, a stretchable gel electrolyte is expected to show high mechanical compatibility with the stretchable electrochromic electrode, and the lasting moisturizing traits of the gel can guarantee long-term usability when exposed to the environment. In this work, a durable and stretchable $ZnCl_2$-EG/H_2O-PVA organohydrogel is deployed as the electrolyte in this stretchable electrochromic system, as schematically illustrated in **Figure 3**a. By incorporating the EG into the electrolyte, EG molecules form hydrogen bonds with PVA chains and induce the crystallization of PVA,[30] affording mechanical stretching and twisting (Figure 3c). Besides, the EG humectant could bind and separate water molecules by hydrogen bonds, slowing down water evaporation and keeping the moisturizing effect of the organohydrogel.[31] And the $ZnCl_2$ as the salt exhibits the advantages of low-cost, high conductivity, and good chemical compatibility in the EG/H_2O-PVA gel system.[32] During optimization, it is found that the $ZnCl_2$-EG/H_2O-PVA organohydrogel with a volume ratio (EG/H_2O) of 1:2 maintains the high conductivity (10.2 mS cm^{-1}) of the pure $ZnCl_2$-PVA hydrogel (14.7 mS cm^{-1}), whereas increasing the ratio of EG/H_2O (2:1) will sacrifice the conductivity of the organohydrogel (2.8 mS cm^{-1}) (Figure S3, Supporting Information). This $ZnCl_2$-EG/H_2O (1:2)-PVA organohydrogel keeps 71% of its initial weight and high conductivity of 4.3 mS cm^{-1} for 12 days in ambient conditions (25 °C and 65% humidity) as illustrated in Figure 3b. In addition, the organohydrogel shows a high transmittance (≈93%) over a wide range of wavelengths (350–950 nm) in Figure 3c, which is beneficial to its application in the electrochromic display. Correspondingly, this transparent $ZnCl_2$-EG/H_2O (1:2)-PVA organohydrogel can endure mechanical deformation and holds long-lasting moisture with high conductivity. It is anticipated that the stretchable electrochromic electrode, integrating with this organohydrogel electrolyte, will exhibit high performances upon stretching deformation and a long cycling lifetime.

2.4. Electrochromic Performances of Stretchable Electrochromic Electrode under Strain

The electrochromic performances of the WO_3 electrode are evaluated with the Zn electrode and carbon cloth parallelly integrated and topped with $ZnCl_2$-EG/H_2O-PVA organohydrogel, according to the illustration in Figure 1. The incorporation of the Zn electrode with the organohydrogel electrolyte provides an effective interfacial construction that suppresses the zinc dendrite growth and hydrogen evolution in this electrochemical device.[33] Then by connecting the WO_3/Zn electrodes, the WO_3 electrode exhibits the self-colored state; by disconnecting the WO_3/Zn electrodes, the O_2 oxidizes the colored electrochromic materials, resulting in the self-bleached state. The stark optical contrast between self-colored/bleached states shows great potential in reflective/non-emissive display applications.[34] To evaluate the feasibility of these electrodes, the reflectance spectra of the stretchable WO_3 electrode are measured, where the reflectance in the initial state of the WO_3 electrode is normalized to 100% as the baseline. Figure S4, Supporting Information compares the baseline with the colored state (the original reflectance spectra of the WO_3 electrode in bleached/colored states are also provided for reference in Figure S4, Supporting Information), where a large reflectance contrast is observed in the broad range of 580–780 nm. The switching behavior of the WO_3-based electrochromic materials is always investigated in this wavelength range, where 633 nm is used

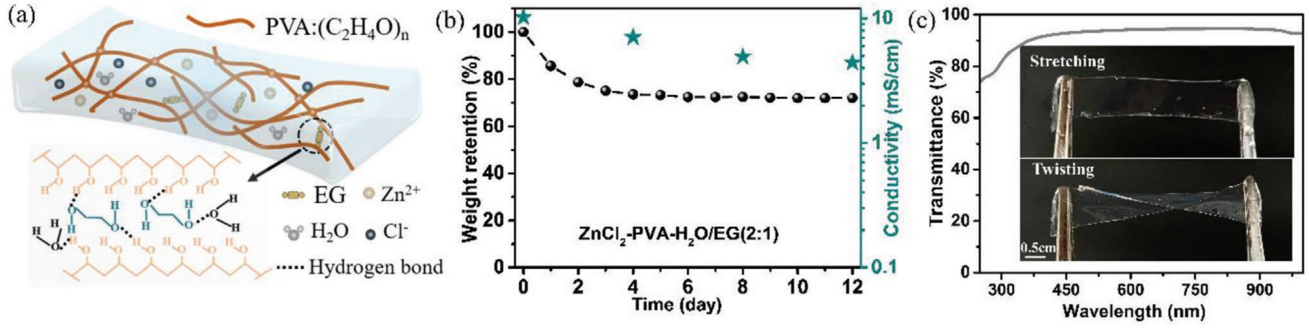

Figure 3. a) Schematic illustration of the stretchable $ZnCl_2$-EG/H_2O-PVA gel electrolyte, b) the weight retention and conductivity change of the gel electrolyte after being exposed to the air in ambient conditions (65% RH, 25 °C), c) the transmittance of gel electrolyte, the stretched/twisted states of the gel electrolyte are shown in the inset.

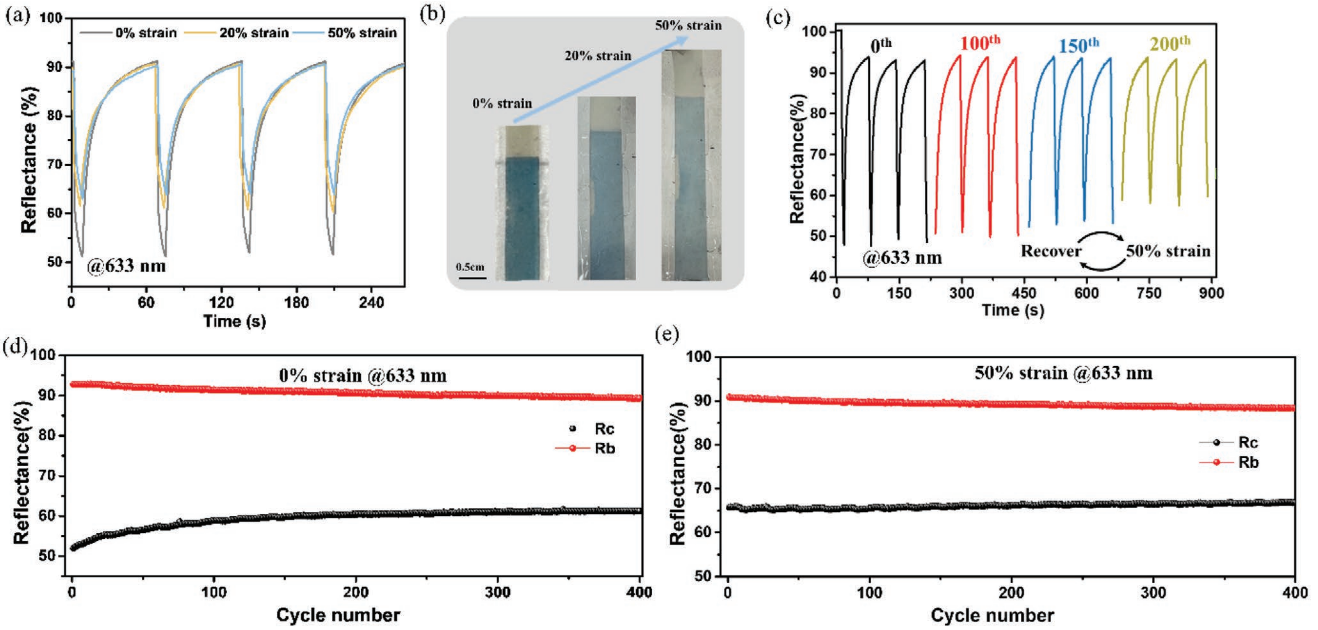

Figure 4. a) The stable in situ reflectance response (2th–5th) and b) corresponding photos of the colored electrochromic electrode at 0%/20%/50% strain states, c) the in situ reflectance response of the electrochromic electrode under repeated stretching/recovery cycles between 0% and 50% strain, the cycling stability of the electrochromic electrode at d) 0% strain and e) 50% strain.

in most cases.[35] Stable in situ reflectance switching behaviors of the stretchable WO_3 electrode are measured at 633 nm by connecting (self-coloring) with the Zn electrode for 6 s and disconnecting (self-bleaching) with the Zn electrode for 60 s at different strain states. Setting the bleaching time to 60 s to obtain the bleached state with ≈90% reflectance rather than the initial state is a strategy that balances the time efficiency and optical properties of the electrochromic electrode, which is expected to be improved in future works for excellent overall performance devices. The electrode is stretched by the stretching mold (detailed schematic diagrams in Figure S5, Supporting Information) to fit the UV–vis spectrophotometer chamber for testing. As shown in **Figure 4**a, the reflectance contrast is about 40% under the 0% strain state. The reflectance contrast decreases with the increasing stretch, where the contrast of 30% and 27% are obtained at 20% and 50% strain states, respectively. The reflectance of the colored states increases during stretching because the increased resistance of the electrode causes a slow electrochemical reaction and the mechanical stretching causes a more sparsely distributed WO_3 layer with a lighter blue color. The corresponding photos of the colored WO_3 electrode at 0%/20%/50% strain states are shown in Figure 4b, illustrating that the stretchable electrochromic electrode could still operate under strain. The response time is then calculated as the time for 90% of the reflectance contrast during coloring/bleaching.[36] The coloring response time increases during the stretching (2.5 s for 0% strain, 4 s for 20% strain, and 4.7 s for 50% strain) and the bleaching response time slightly changes (between 35 and 36 s) upon stretching, which is owning to the increase in resistance of the electrochromic electrode, slowing down the electrochromic reaction speed and the response speed of the device. To more clearly illustrate the electrochromic effect of the electrode, the contribution of the protection PEDOT:PSS layer is analyzed, showing a slight electrochromic performance of 5% contrast at 633 nm (Figure S6, Supporting Information). The number of spray coating layers of the WO_3 electrode is investigated with 6–20 spray layers. The WO_3 electrode with the above electrochromic properties is based on the optimum spray coating layers of 12–14 layers. A thick WO_3 (20 layers) would induce high resistance to the electrode resulting in a slower electrochromic reaction (Figure S7, Supporting Information). On the contrary, a thin WO_3 (6 layers) would exhibit a limited electrochromic performance with a smaller reflectance contrast (Figure S8, Supporting Information).

To verify the mechanical durability of the electrode, this electrochromic electrode was repeatedly stretched (50% strain) and recovered for 200 cycles, showing a reversible color/bleach performance and keeping 81% retention of its initial reflectance (Figure 3c). The electrochromic electrode at unstretched and stretched (50%) states could also maintain 70% and 85% of their initial reflectance contrast after 400 continuous coloring/bleaching cycles without any power consumption, suggestive of excellent electrochemical stability. More importantly, this stretchable WO_3 electrochromic electrode with self-powered mode shows an overall comparable performance with other stretchable/foldable WO_3-based electrochromic electrodes without self-powering capability[4,12,37] and those with flexible self-powered WO_3-based electrochromic electrodes,[22] as shown in Table S1, Supporting Information.

2.5. The Self-Coloring and Self-Bleaching Mechanisms of the Electrochromic Device

To reveal the self-powered mechanism in this electrochromic system, an energy level transition diagram is constructed in

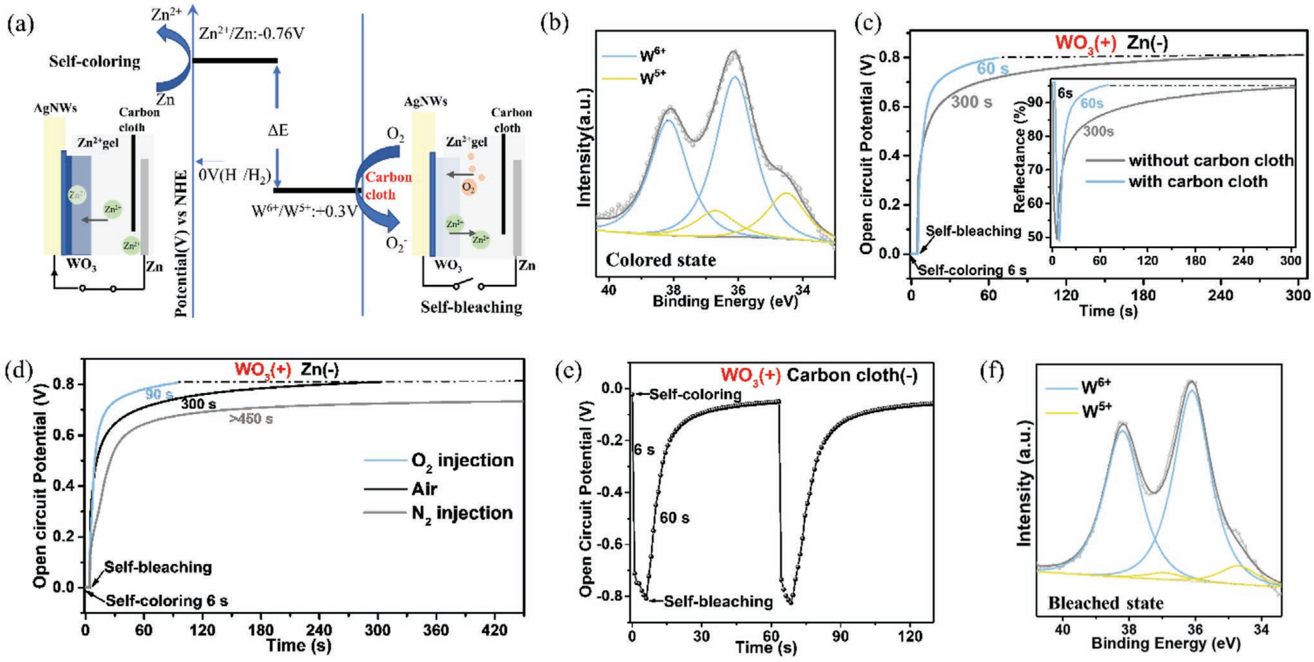

Figure 5. a) The schematic illustration and corresponding energy level transition diagram of self-coloring/self-bleaching mechanisms, b) the XPS spectra of the W element of the WO_3 film in the colored state, c) the open-circuit potential between the WO_3 electrode and Zn electrode during self-coloring/bleaching with/without the carbon cloth, the inset shows the corresponding optical properties of the WO_3 electrode, d) the open-circuit potential between the WO_3 electrode and Zn electrode during self-coloring/bleaching in Air or with O_2/N_2 injection, e) the open-circuit potential between the WO_3 electrode and carbon cloth during self-coloring/bleaching, f) the XPS spectra of W element of the WO_3 film in the bleached state.

Figure 5a. During the coloration process (when two electrodes are connected), the work function difference between the Zn electrode ($Zn^{2+}/Zn = -0.76$ V vs standard hydrogen electrode (SHE)) and WO_3 electrode ($W^{6+}/W^{5+} = 0.3$ V vs SHE) would drive Zn to release electrons, forming Zn^{2+} ions into the electrolyte. Meanwhile, the WO_3 electrode would spontaneously receive these electrons from the circuit alongside the concomitant intercalation of Zn^{2+} ions, leading to the reduction of W^{6+} to W^{5+}. The self-coloring process can be elaborated by the following electrochemical reactions:

$$\text{Zn electrode: } Zn - 2e^- \rightarrow Zn^{2+} \quad (1)$$

$$WO_3\text{ electrode: } WO_3 + \alpha Zn^{2+} + 2\alpha e^- \rightarrow Zn_\alpha WO_3 \quad (2)$$

The valence transition of the W element during the reaction was further evidenced by the X-ray photoelectron spectroscopy (XPS) measurements. The peaks at 38.2 and 36.1 eV correspond to the binding energies of W^{6+} $4f_{5/2}$ and $4f_{7/2}$ species, and the peaks at 36.9 and 34.7 eV are assigned to the W^{5+} $4f_{5/2}$ and $4f_{7/2}$ species due to the reduction process. The relative quantity of W^{5+} in W species (W^{5+} and W^{6+}) increases from 6.8% in the initial state (Figure S9, Supporting Information) to 23.1% in the colored state (Figure 5b). These values are in the reasonable range when compared with the reported literature.[38] Moreover, the open circuit potential between the WO_3 electrode and Zn electrode (Figure 5c) was tested to reveal the chemical potential variation of the WO_3 electrode with ion-insertion/extraction during the self-coloring/bleaching process,[39] which was associated with the optical properties of the WO_3 electrode inside in Figure 5c. When the two electrodes are connected/disconnected, the WO_3 undergoes the self-coloring/bleaching process with decreasing/increasing reflectance. In this case, there is an open circuit potential of 0.8 V between the fully bleached WO_3 electrode and Zn electrode, providing the driving force for the subsequent self-coloring process.

As for the self-bleaching process, the O_2 plays a critical role in oxidizing the colored WO_3 to the bleached state. In this electrochromic system, the organohydrogel electrolyte is assembled on top, which provides a large open area for air/oxygen to diffuse into the electrolyte. During oxidation, oxygen molecules trap the electrons from reduced WO_3[40] and are directly in contact with the surface of the WO_3 film. In this case, the larger surface roughness of the WO_3 film (Figure 2f) is expected to promote the self-bleaching behavior.[41] The corresponding Equation (3) for bleaching is shown below:

$$Zn_\alpha WO_3 + O_2 \rightarrow WO_3 + \alpha Zn^{2+} + O^{2-} \quad (3)$$

The role of oxygen in this self-bleaching reaction was proved by regulating the oxygen content of the atmosphere in the sealed box for device testing. As shown in Figure 5d, higher oxygen content can lower the self-bleaching time to as short as 90 s. Unlike in an oxygen-saturated condition, the self-bleaching process slows down to 300 s in ambient conditions due to the low rate of oxygen diffusivity into the electrolyte. Improving the self-bleaching rate in the ambient environment without complicated oxygen regulating set-up is crucial because it could not only avoid the oxidation of AgNWs substrate in high content of oxygen but also simplify the use of the device for promising futuristic applications.

Herein, a carbon cloth electrode is simply integrated into this system, which is placed parallel to the electrochromic electrode and indirectly connected to the electrochromic electrode by the common upper organohydrogel layer. With the addition of the carbon cloth electrode, a faster self-bleaching behavior of the WO_3 electrode is exhibited in Figure 5c, to which bleaching time is reduced from 300 s (without carbon cloth) to 60 s (with carbon cloth) at the wavelength of 633 nm. Furthermore, the role of carbon cloth is elucidated from the perspective of charge transfer inside the electrochromic device during the self-bleaching process. It is known that the oxygen molecules at the interface between the electrolyte and WO_3 electrode have already trapped most of the electrons over a large surface area of the reduced WO_3 electrode. As shown in Figure 5e, the carbon cloth electrode displays a more positive potential (≈0.8 V) than the fully reduced WO_3 electrode, which can directly extract the trapped electrons out of the WO_3 electrode via the leakage current between the two electrodes. To further clarify this conclusion, we test the chronoamperometry curves (Figure S10, Supporting Information) under the condition that connects the WO_3/carbon cloth electrodes for bleaching and connects the WO_3/Zn electrodes for coloring to derive the leakage current between the WO_3/carbon cloth electrodes with the disconnected states. It is calculated that the charge extracted from the WO_3 electrode through the external circuit connected to the carbon cloth electrode only accounts for 25% of the charge inserted into the WO_3 electrode connected to the Zn electrode. With that, the electrochromic performance improvement by connecting the WO_3/carbon cloth electrodes for self-bleaching is limited as shown in the corresponding reflectance changes in Figure S10, Supporting Information. Therefore, in the case of bleaching by disconnecting the WO_3/carbon cloth electrodes, the charge extraction is caused by the leakage current inside the electrochromic device. Given that when the reduced WO_3 electrode is oxidized to the bleached state, the valance transition from W^{5+} to W^{6+} is realized. It is verified by the XPS measurements that the ratio of W^{5+} in W species (W^{5+} and W^{6+}) is decreased from 23.1% in the colored state to 7.6% in the bleached state (Figure 5f). In this case, the Zn^{2+} ions will diffuse out of the WO_3 electrode during the bleaching process due to the charge balance inside the bleached WO_3 electrode. And the Zn^{2+} ions will not be converted into Zn, the consumption of Zn exists but is negligible due to the thin WO_3 film with a diminutive mass.

2.6. Application of Self-Powered and Light-Adaptable Stretchable Electrochromic Display

Benefitting from the self-powered (self-coloring/bleaching) features, the stretchable electrochromic device can be employed to construct a promising reflective display with zero power consumption, which is highly sought-after for futuristic portable electronics. In most cases, the electrochromic display exhibits high visibility under bright conditions by utilizing the reflection of ambient light, but its use is hindered under dark conditions with the absence of light sources.[34] To explore its applicability in every light condition, the phosphorescent stretchable substrate is being deployed here serving as the "backlight" under dark conditions. As a proof of concept, a light-adaptable electrochromic display with the phosphorescent substrate (9 cm × 3 cm) has been assembled and is shown in **Figure 6**a. Under a bright environment, the patterned electrochromic "ECD" electrodes regulate the reflection of ambient light by simply connecting/disconnecting the Zn electrode. In the meantime, the phosphorescent substrate absorbs and converses the energy of the visible light. Under a dark condition, the conversed energy is then gradually released as greenish blue phosphorescence, where the "ECD" pattern is in the "on" state by blocking the emitted phosphorescence. The corresponding electrochromic function of the displays is shown in Figure 6b. By referencing the reflectance in the initial state of the display @633 nm, the stable "on" (colored) state (46.8% @633 nm) of the display can be maintained for at least 30 min by connecting the WO_3 /Zn electrodes. Subsequently, this colored WO_3 electrode is disconnected from the Zn electrode, exhibiting the stable "off" (bleached) state (100% @633 nm) for more than 30 min without the concern that the ions inserted in the electrode for a long time cannot be extracted. It ensures the continuous display ability with large optical contrast of the display without any power input. Moreover, the stretchability of the display was also demonstrated in Figure S11, Supporting Information, where the "ECD" pattern of the display is still visible at 35% strain state under bright/dark conditions. Besides, the phosphorescent lifetime of the displays is investigated after being exposed to the light for 12 h (similar to the daytime). When the light irradiation is terminated, the phosphorescent substrate spontaneously emits light with a broad wavelength which peaked at 498 nm as shown in Figure 6c. There is an emission intensity contrast between the "on/off" states because the colored electrochromic part could block the emitted light which helps to distinguish the pattern. Over time, the emission intensity of the phosphorescent substrate would decrease as the stored energy is slowly depleting in the form of light.[42] Because of that, the prototype shows only a faint display effect after 20 min in the dark as shown in Figure S12, Supporting Information. Furthermore, the spray-coating fabrication method of the electrochromic layer enables it to desired patterns. As shown in Figure 6d, the light-adaptable electrochromic display (3.5 cm × 4 cm) exhibits the transition from the "off" to "on" states with flower patterns under both bright and dark conditions without power input. Overall, this is the first stretchable display that exhibits its promising application prospects in various scenarios for outdoor use without an external power source.

3. Conclusion

In this work, we have successfully demonstrated a novel self-powered stretchable electrochromic display assembled by different functional layers. The PEDOT:PSS/AgNWs/PDMS stretchable conductor ensures excellent conductive properties against mechanical stretching and peeling, in which the PEDOT:PSS layer functions as the binding layer for stronger adhesion and conductivity. By integrating the transparent and

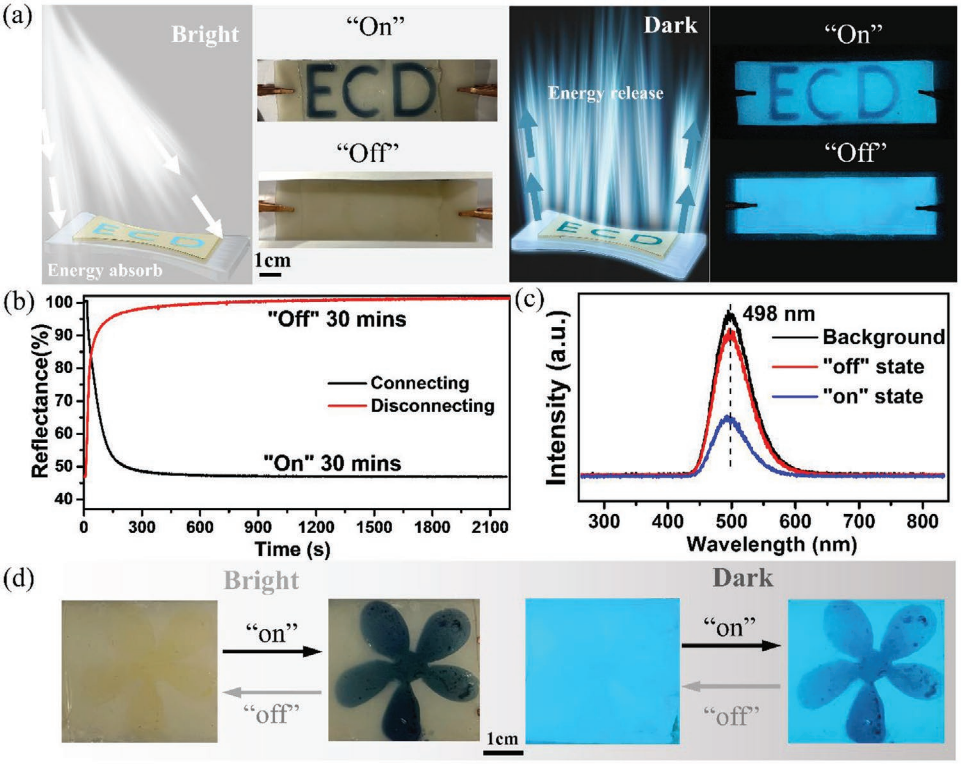

Figure 6. a) The schematic diagram and photos of the light-adaptable stretchable electrochromic display in "on/off" states in dark/bright conditions with the "ECD" pattern, b) the electrochromic performances of the display in "on/off" states, c) the emission intensity of the display in "on/off" states in dark conditions, d) the photos of the flower-patterned light-adaptable electrochromic display.

stretchable $ZnCl_2$-EG/H_2O (1:2)-PVA organohydrogel as the top layer, the WO_3 on the conductor as the stretchable electrochromic electrode exhibits its reversible self-coloring/bleaching performances upon stretching when assembled in parallel with the carbon cloth and zinc electrodes. When connecting the Zn/WO_3 electrodes, the self-coloring is achieved by the chemical potential gap between Zn/WO_3 electrodes; when disconnecting the Zn/WO_3 electrodes, the self-bleaching is exhibited due to the oxidation of reduced WO_3 electrode by dissolved O_2 in electrolyte and is facilitated by the leakage current inside the carbon cloth/WO_3 electrodes. Furthermore, the stable mechanical and electrochemical properties of the stretchable electrode are also shown upon 200 stretching/recovery cycles and 400 coloring/bleaching cycles without electrical consumption. The as-prepared device combined with a phosphorescent substrate shows its promising application for light-adaptable electrochromic display. This stretchable display exhibits the "on/off" (colored/bleached) states without an external power source and is applicable in every light condition, which provides new possibilities for futuristic multifunctional stretchable and portable display electronics.

4. Experimental Section

Materials: Silicon dioxide nanopowder (5–10 nm particle size), $ZnCl_2$, PVA polymer ($M_w \approx 130\,000$, hydrogen peroxide solution (30% H_2O_2)), tungsten powder, and mono ethylene glycol (EG) were purchased from Sigma-Aldrich. The commercial silver nanowires (AgNWs) were bought from Nanjing XFNANO Materials Co., Ltd with diameters of 50 nm and lengths of 100–200 µm. PEDOT: PSS (PH 1000) was purchased from Ossila Ltd. The commercial phosphorescent paint materials were obtained from Shanghai Zhendi New Material Technology Co., Ltd. Carbon cloth (WOS 1009) was purchased from CeTech Co., Ltd.

Preparation of the Stretchable Electrochromic Electrode: First, the AgNWs/PDMS substrate was prepared by the reported method:[12] the commercial AgNWs were diluted in isopropanol solution (1 mg mL^{-1}). The glass substrates were cleaned in acetone, de-ionized water, and isopropanol solution with 15 min sonication, respectively. Then the diluted AgNWs solution was spray-coated onto the glass substrate using a spray gun in the fume hood. Then the SiO_2 suspension with a concentration of 3.5 wt% in ethanol was spin-coated onto the AgNWs/glass surface (1000 rpm, 50 s). The PDMS was prepared by mixing the base and curing agent (Sylgard 184, Dow Corning) with a ratio of 10:1. The PDMS mixture was poured onto the AgNWs/glass substrate and cured at 80 °C for 2 h. Then the sample was immersed in de-ionized water at 50 °C for 30 min. Therefore, the AgNWs/PDMS substrate was successfully peeled from the glass substrate. Next, the PEDOT:PSS solution was diluted in IPA with a concentration of 10 wt%, then the prepared PEDOT:PSS solution was spray-coated onto the AgNWs/PDMS substrate for two layers at a spray rate of 0.03 mL s^{-1} and a spray distance of 15 cm, where 5 s spraying for each layer was followed by a 10 s delay between layers. Then the sample was heated at 120 °C (vacuum state) for 30 min for PEDOT:PSS curing. The WO_3 precursor solution was prepared in our previous report:[43] Tungsten powder was reacted with hydrogen peroxide solution (30% H_2O_2) in a water bath (100 °C) for 5 h, then the product was dried in the vacuum oven (100 °C) overnight. The resulting residue was ground and ultrasonically dispersed in IPA with a concentration of 0.25 wt%. Then the pale yellow WO_3 precursor was obtained after filtering (Figure S13, Supporting Information). After that, the electrochromic electrode was prepared by spraying the WO_3 precursor for 12–14 layers with the same above spray parameters. Then the electrode was dried at 120 °C (vacuum state) for 30 min.

As for the light-adaptable electrochromic display, the conductive phosphorescent substrate was integrated with the electrochromic electrode. The conductive phosphorescent substrate was fabricated by following steps: first, a thin layer of PDMS was spin-coated (800 rpm, 5 s) into the spray-coated AgNWs-glass substrate and cured. The commercial phosphorescent paint materials, the PDMS base, and the curing agent were mixed with a weight ratio of 2:10:1. Then the mixed phosphorescent materials were poured into the top of the thin PDMS-AgNWs-glass substrate, degassed, and cured at 80 °C for 2 h. After the same water bath treatment, the conductive phosphorescent substrate was obtained after peeling from the glass substrate.

Preparation of the Stretchable Electrolyte: The PVA polymer was dissolved and stirred mixed with 9 g EG/H_2O binary solvent (1:2/2:1/0:1, v/v) in an oil bath (95 °C) for 2 h. Then 1.363 g (0.1 mol) $ZnCl_2$ was added and stirred into the solution for 1 h. The sticky solution was poured into a glass mold and placed at -20 °C for 2 h. After that, a transparent PVA/EG-$ZnCl_2$ gel was obtained.

Fabrication of the Electrochromic Device: The Zn electrode, WO_3 electrochromic electrode, and carbon cloth electrode were placed in parallel, then the electrolyte gel was assembled on top of the electrodes.

Characterization: The resistance of the electrodes upon stretching was tested by a motorized forced test stand (ESM303, Mark-10) with a speed of 2 mm min^{-1}. The chronoamperometry curves of the electrochromic device and the electrochemical impedance spectroscopy (EIS) of the gel electrolyte were performed using an Autolab PGSTAT30, where the gel electrolyte was sandwiched by two copper plates during the test. Then the conductivity of the electrolyte is calculated by the $\sigma = l/RS$. l, S, and R represent the thickness, cross-section area, and resistance of the gel, respectively. The transmittance of the gel electrolyte and the reflectance of the electrochromic devices were recorded using the UV–vis NIR Spectrophotometer (Lambda 950). In the reflective mode, the integrating sphere was inside to gather the reflective signal. And the cycling test of the device was combined with the self-customized time-controllable switch (Figure S14, Supporting Information), which controls the connecting/disconnecting time of the device. The open-circuit potential of the WO_3 electrode and carbon cloth/Zn electrodes was tested by the digital multimeter (DAQ6510, Keithley). The atmosphere regulating the oxygen content for the device was conducted in a self-made sealed box by injecting the O_2/N_2 flow for 10 min with 5 psi before testing. Emission from the phosphorescent-PDMS substrate was recorded by an optical fiber with an Acton SP-2300 monochromator. Then the spectrum was tested by a Princeton Pixis 100B spectroscopy CCD detector. The microstructure and element mapping of the electrodes were conducted by the SEM (FE-SEM, JSM 7600F). The crystal structure of the WO_3 film was measured by X-ray diffraction (Shimadzu XRD-6000, Cu Kα X-ray). The element analysis of the WO_3 film was characterized by the X-ray photoelectron spectrometer (Physical Electronics Inc. Quantera II). The surface roughness of the WO_3 film was tested by atomic force microscopy (AFM, Asylum Research Cypher S).

Supporting Information

Supporting Information is available from the Wiley Online Library or from the author.

Acknowledgements

This work was supported by funding from the Ministry of Education (MOE) Singapore, AcRF Tier 1, Project No. RG64/21 and National Natural Science Foundation of China (No. 51902250). The author W.W. thanks the support from the China Scholarship Council (Grant No. 202006280507) and Basic Scientific Research of Xi'an Jiaotong University (Grant No. xzy022022028).

Conflict of Interest

The authors declare no conflict of interest.

Data Availability Statement

The data that support the findings of this study are available from the corresponding author upon reasonable request.

Keywords

electrochromic displays, light-adaptable, self-powered, stretchable electronics, tungsten oxide

Received: November 30, 2022
Revised: February 5, 2023
Published online:

---

[1] U. Linderhed, I. Petsagkourakis, P. A. Ersman, V. Beni, K. Tybrandt, *Flexible Printed Electron* **2021**, *6*, 045014.
[2] a) C. Yan, W. Kang, J. Wang, M. Cui, X. Wang, C. Y. Foo, K. J. Chee, P. S. Lee, *ACS Nano* **2014**, *8*, 316; b) H. Park, D. S. Kim, S. Y. Hong, C. Kim, J. Y. Yun, S. Y. Oh, S. W. Jin, Y. R. Jeong, G. T. Kim, J. S. Ha, *Nanoscale* **2017**, *9*, 7631.
[3] H. Fang, Z. Zhao, W. Wu, H. Wang, *J. Inorg. Mater.* **2021**, *36*, 140.
[4] T. G. Yun, M. Park, D. H. Kim, D. Kim, J. Y. Cheong, J. G. Bae, S. M. Han, I. D. Kim, *ACS Nano* **2019**, *13*, 3141.
[5] T. Hao, S. Wang, H. Xu, X. Zhang, J. Xue, S. Liu, Y. Song, Y. Li, J. Zhao, *Chem. Eng. J.* **2021**, *426*, 130840.
[6] Q. Liu, Z. Xu, W. Qiu, C. Hou, Y. Wang, P. Yao, R. Yu, W. Guo, X. Y. Liu, *RSC Adv.* **2018**, *8*, 18690.
[7] H. Kai, W. Suda, Y. Ogawa, K. Nagamine, M. Nishizawa, *ACS Appl. Mater. Interfaces* **2017**, *9*, 19513.
[8] P. Zhao, H. Chen, B. Li, H. Tian, D. Lai, Y. Gao, *Opt. Mater.* **2019**, *94*, 378.
[9] J. Sun, X. Pu, M. Liu, A. Yu, C. Du, J. Zhai, W. Hu, Z. L. Wang, *ACS Nano* **2018**, *12*, 6147.
[10] H. Fan, K. Li, Q. Li, C. Hou, Q. Zhang, Y. Li, W. Jin, H. Wang, *J. Mater. Chem. C* **2017**, *5*, 9778.
[11] a) C. Yan, J. Wang, X. Wang, W. Kang, M. Cui, C. Y. Foo, P. S. Lee, *Adv. Mater.* **2014**, *26*, 943; b) S. Yao, Y. Zhu, *Adv. Mater.* **2015**, *27*, 1480.
[12] G. Cai, S. Park, X. Cheng, L. S. Eh, P. S. Lee, *Sci. Technol. Adv. Mater.* **2018**, *19*, 759.
[13] W. Guo, Z. Cong, Z. H. Guo, P. Zhang, Y. Chen, W. Hu, Z. L. Wang, X. Pu, *Adv. Funct. Mater.* **2021**, *31*, 2104348.
[14] J. Wang, L. Zhang, L. Yu, Z. Jiao, H. Xie, X. W. Lou, X. W. Sun, *Nat. Commun.* **2014**, *5*, 4921.
[15] a) W. Wu, H. Fang, H. Ma, L. Wu, Q. Wang, H. Wang, *ACS Appl. Mater. Interfaces* **2021**, *13*, 20326; b) X. Li, Z. Du, Z. Song, B. Li, L. Wu, Q. Liu, H. Zhang, W. Li, *Adv. Funct. Mater.* **2018**, *28*, 1800599.
[16] J. Zhao, Y. Tian, Z. Wang, S. Cong, D. Zhou, Q. Zhang, M. Yang, W. Zhang, F. Geng, Z. Zhao, *Angew. Chem., Int. Ed.* **2016**, *55*, 7161.
[17] Y. Tian, W. Zhang, S. Cong, Y. Zheng, F. Geng, Z. Zhao, *Adv. Funct. Mater.* **2015**, *25*, 5833.

[18] H. Li, L. McRae, C. J. Firby, A. Y. Elezzabi, *Adv. Mater.* **2019**, *31*, 1807065.

[19] Y. Zhai, Y. Li, Z. Zhu, C. Zhu, D. Du, Y. Lin, *ACS Appl. Mater. Interfaces* **2019**, *11*, 48013.

[20] Y. Zhai, Y. Li, H. Zhang, D. Yu, Z. Zhu, J. Sun, S. Dong, *ACS Appl. Mater. Interfaces* **2019**, *11*, 28072.

[21] Y. Luo, H. Jin, Y. Lu, Z. Zhu, S. Dai, L. Huang, X. Zhuang, K. Liu, L. Huang, *ACS Energy Lett.* **2022**, *7*, 1880.

[22] J.-L. Wang, S.-Z. Sheng, Z. He, R. Wang, Z. Pan, H.-Y. Zhao, J.-W. Liu, S.-H. Yu, *Nano Lett.* **2021**, *21*, 9976.

[23] W. Wu, H. Fang, H. Ma, L. Wu, W. Zhang, H. Wang, *Nano-Micro Lett.* **2020**, *13*, 20.

[24] a) K.-H. Heckner, A. Kraft, *Solid State Ionics* **2002**, *152–153*, 899; b) Y. Gui, D. J. Blackwood, *J. Electrochem. Soc.* **2014**, *161*, E191; c) Y. Guo, W. Li, H. Yu, D. F. Perepichka, H. Meng, *Adv. Energy Mater.* **2017**, *7*, 1601623.

[25] J. Lee, P. Lee, H. B. Lee, S. Hong, I. Lee, J. Yeo, S. S. Lee, T.-S. Kim, D. Lee, S. H. Ko, *Adv. Funct. Mater.* **2013**, *23*, 4171.

[26] a) V. V. Kondalkar, R. R. Kharade, S. S. Mali, R. M. Mane, P. B. Patil, P. S. Patil, S. Choudhury, P. N. Bhosale, *Superlattices Microstruct.* **2014**, *73*, 290; b) S. Poongodi, P. S. Kumar, D. Mangalaraj, N. Ponpandian, P. Meena, Y. Masuda, C. Lee, *J. Alloys Compd.* **2017**, *719*, 71.

[27] J. Zhang, J. P. Tu, G. F. Cai, G. H. Du, X. L. Wang, P. C. Liu, *Electrochim. Acta* **2013**, *99*, 1.

[28] J. Han, K.-w. Ko, S. Sarwar, M.-s. Lee, S. Park, S. Hong, C.-h. Han, *Electrochim. Acta* **2018**, *278*, 396.

[29] a) M. Wang, X. Xing, I. F. Perepichka, Y. Shi, D. Zhou, P. Wu, H. Meng, *Adv. Energy Mater.* **2019**, *9*, 1900433; b) Q. Chen, Y. Shi, K. Sheng, J. Zheng, C. Xu, *ACS Appl. Mater. Interfaces* **2021**, *13*, 56544; c) W. C. Poh, A. L.-S. Eh, W. Wu, X. Guo, P. S. Lee, *Adv. Mater.* **2022**, *34*, 2206952.

[30] Q. Rong, W. Lei, J. Huang, M. Liu, *Adv. Energy Mater.* **2018**, *8*, 1801967.

[31] Y. Li, H. Chengxin, J. Lan, B. Yan, Y. Zhang, L. Shi, R. Ran, *Polymer* **2020**, *186*, 122027.

[32] a) H. M. Trimble, *Ind. Eng. Chem.* **1931**, *23*, 165; b) Q. Zhang, Y. Ma, Y. Lu, L. Li, F. Wan, K. Zhang, J. Chen, *Nat. Commun.* **2020**, *11*, 4463.

[33] a) L. Wang, W. Huang, W. Guo, Z. H. Guo, C. Chang, L. Gao, X. Pu, *Adv. Funct. Mater.* **2022**, *32*, 2108533; b) L. Ma, C. Zhi, *Electrochem. Commun.* **2021**, *122*, 106898.

[34] M. Pietsch, T. Rödlmeier, S. Schlisske, J. Zimmermann, C. Romero-Nieto, G. Hernandez-Sosa, *J. Mater. Chem. C* **2019**, *7*, 7121.

[35] a) D. S. Dalavi, R. S. Devan, R. A. Patil, R. S. Patil, Y.-R. Ma, S. B. Sadale, I. Kim, J.-H. Kim, P. S. Patil, *J. Mater. Chem. C* **2013**, *1*, 3722; b) D. Ma, G. Shi, H. Wang, Q. Zhang, Y. Li, *J. Mater. Chem. A* **2013**, *1*, 684.

[36] W. Wu, L. Wu, H. Ma, L. Wu, H. Wang, H. Fang, *Chem. Eng. J.* **2022**, *446*, 137122.

[37] W. Kang, C. Yan, C. Y. Foo, P. S. Lee, *Adv. Funct. Mater.* **2015**, *25*, 4203.

[38] a) R. Iimura, T. Hasegawa, S. Yin, *Inorg. Chem.* **2022**, *61*, 2509; b) G. Leftheriotis, S. Papaefthimiou, P. Yianoulis, A. Siokou, *Thin Solid Films* **2001**, *384*, 298; c) Y. F. Lu, H. Qiu, *J. Appl. Phys.* **2000**, *88*, 1082.

[39] a) J. Bisquert, *Electrochim. Acta* **2002**, *47*, 2435; b) Q. Liu, G. Dong, Q. Chen, J. Guo, Y. Xiao, M.-P. Delplancke-Ogletree, F. Reniers, X. Diao, *Sol. Energy Mater. Sol. Cells* **2018**, *174*, 545.

[40] M. Miyauchi, Y. Li, S. Yanai, K. Yotsugi, *Chem. Commun.* **2011**, *47*, 8596.

[41] J.-G. Zhang, D. Benson, C. E. Tracy, J. Webb, S. Deb, *Self-Bleaching Mechanism of Electrochromic* WO_3*Films*, Vol. *2017*, SPIE, Bellingham, Washington **1993**.

[42] Y. Yin, H. Chen, X. Zhao, W. Yu, H. Su, Y. Chen, P. Lin, *Energy Convers. Manage.* **2022**, *266*, 115804.

[43] H. Fang, P. Zheng, R. Ma, C. Xu, G. Yang, Q. Wang, H. Wang, *Mater. Horiz.* **2018**, *5*, 1000.